Catalysis Letters Vol. 113, Nos. 1–2, January 2007 (© 2007)
DOI: 10.1007/s10562-006-9003-7

In situ time-resolved characterization of novel Cu–MoO_2 catalysts during the water–gas shift reaction

Wen Wen,[a] Liu Jing,[a] Michael G. White,[a] Nebojsa Marinkovic,[b] Jonathan C. Hanson,[a] and José A. Rodriguez[a,]*

[a]*Chemistry Department, Brookhaven National Laboratory, Upton, NY 11973, USA*
[b]*Department of Chemical Engineering, University of Delaware, Newark, DE 19716, USA*

Received 12 October 2006; accepted 24 November 2006

A novel and active Cu–MoO_2 catalyst was synthesized by partial reduction of a precursor $CuMoO_4$ mixed-metal oxide with CO or H_2 at 200–250 °C. The phase transformations of Cu–MoO_2 during H_2 reduction and the water–gas shift reaction could be followed by *in situ* time resolved XRD techniques. During the reduction process the diffraction pattern of the $CuMoO_4$ collapsed and the copper metal lines were observed on an amorphous material background that was assigned to molybdenum oxides. During the first pass of water–gas shift (WGS) reaction, diffraction lines for $Cu_6Mo_5O_{18}$ and MoO_2 appeared around 350 °C and $Cu_6Mo_5O_{18}$ was further transformed to Cu/MoO_2 at higher temperature. During subsequent passes, significant WGS catalytic activity was observed with relatively stable plateaus in product formation around 350, 400 and 500 °C. The interfacial interactions between Cu clusters and MoO_2 increased the water–gas shift catalytic activities at 350 and 400 °C.

KEY WORDS: water–gas shift; copper; molybdenum oxides; $CuMoO_4$; H_2; water; CO; CO_2; X-ray diffraction; X-ray absorption spectroscopy.

1. Introduction

With the increasing demand for fossil fuels, alternative energy resources are very critical. A promising energy source is hydrogen that is environmentally friendly and renewable. The industrial mass production of hydrogen is primarily from steam gas reforming of methane to produce CO and H_2. In addition to hydrocarbons from the oil industry (or natural gas), new raw materials, such as biomass or waste, could also be used for reforming purposes [1].

The water–gas shift (WGS) process provides a means of utilizing the CO for generation of H_2 by reaction of a gas mixture of CO and H_2O. ($CO + H_2O \rightarrow H_2 + CO_2$) Fe–Cr and Zn–Al–Cu oxides are the commercially used catalysts for the water–gas shift reaction at temperatures between 350–500 and 180–250 °C, respectively. However, these oxide catalysts are pyrophoric and are normally required lengthy and complex activation steps before usage [2]. Consequently other catalysts are being sought.

Oxide supported Cu catalysts show significant water–gas shift activity, but are highly depended upon the synthesis conditions used, since these will determine the cluster size and the nature of the active sites [1–5]. Mixed-metal $Ce_{1-x}Cu_xO_2$ oxides have important applications in the water–gas shift reaction [3–5]. A recent study showed some interesting electronic and structural properties for this type of catalysts, where the copper oxide embedded in the cerium oxide could be reduced/oxidized reversibly using reductive/oxidative gas mixtures, respectively [6]. It was further observed via *in situ* time resolved XRD and XAFS that both metallic copper and oxygen vacancies in ceria are involved in the generation of catalytic active sites for the water–gas shift reaction [7]. In this work, we investigated the WGS activity of another mixed-metal oxide that contains copper: $CuMoO_4$. The observation that there is a slight increase on the WGS activity when the mixed metal oxide was partially reduced suggests that a more complete reduction of the mixed metal oxide might produce a more active catalyst. Consequently the catalyst was activated by more complete reduction with pure hydrogen.

In this study, synchrotron-based *in situ* time-resolved X-ray diffraction (TR-XRD) is employed to study the behavior under WGS reaction conditions of $CuMoO_4$ and nanostructured Cu−MoO_2, produced by partial reduction of the mixed-metal oxide. The oxidation states of the elements in the catalysts are examined by means of x-ray absorption near-edge spectroscopy (XANES). For the first time, a novel Cu–MoO_2 catalyst is synthesized and good activity is achieved for the water–gas shift reaction. This work shows an important interplay of Cu metal and the molybdenum oxide support in the catalysis.

---

*To whom correspondence should be addressed.
E-mail: Rodrigez@bnl.gov

2. Experimental

The *in situ* time-resolved X-ray diffraction patterns were obtained at beam line X7B (λ = 0.922 Å) of the National Synchrotron Light Source (NSLS) at Brookhaven National Laboratory [6–8]. A Mar345 image detector was used to collect two-dimensional powder patterns and the Fit2D code was used to integrate the powder rings.

The copper molybdate ($CuMoO_4$) was purchased from Aldrich (99% purity). The sample (3–4 mg) was loaded into a sapphire capillary tube, which was attached to a flow system [6–9]. The capillary was heated using a small resistance heater that was wrapped around the capillary and a 0.1 mm chromel–alumel thermocouple placed inside the capillary was used to measure the temperature. The Cu–MoO_2 catalyst was synthesized in a flow cell with a H_2 gas stream at 260 °C.

The water–gas shift reaction was carried out isothermally at 350, 400 and 500 °C, with a flow of 5% CO/He gas mixture through a water bubbler at a rate of $\sim$10 ml/min. At each temperature, the water–gas shift reaction was monitored for a period of three hours. During the water–gas shift reaction, the relative ratio of water vapor pressure to CO in the feed gas mixture was adjusted to be around 0.35. The concentrations of the residual gases were measured with a 0–200 amu quadruple mass spectrometer while *in situ* diffraction patterns were collected. Due to the very small amount of catalyst (3–4 mg) in the micro-reactor, our detection set-up was able to detect the products (H_2, CO_2) only at temperatures above 300 °C when the WGS rate was fast. The reaction could be taking place also at temperatures below 300 °C [7].

The Rietveld refinement was performed using EXPGUI/GSAS program [10, 11], where multiple phases could be analyzed.

Cu K-edge and Mo L_{III}-edge XANES spectra were obtained at beamline X19A of the NSLS [12, 13]. The XANES spectra were taken in the "fluorescence yield mode" using a PIPS (passivated-implanted planar silicon) detector. In order to remove the disturbance of higher order harmonics in the beam, the I_0 was detuned 30 % and 70 % for the Cu K-edge and Mo L_{III} edge, respectively. The incident (I_0), transmitted (I_t) and reference (I_{ref}) synchrotron beam intensities were measured simultaneously using gas proportional detectors filled with 100% N_2 gas for the Cu K-edge measurements and 100% helium for the Mo L_{III} edge measurements. XANES data were analyzed using the ATHENA program [14].

3. Results and discussions

First, $CuMoO_4$ was tested for the water–gas shift but only small catalytic activity was observed. During the water–gas shift reaction (shown in figure 1a) the $CuMoO_4$ transformed to three different phases. Around 320 °C, an intermediate phase, which could not be identified, was formed. Next, $Cu_{4-x}Mo_3O_{12}$ [15] was observed at 350 °C. At higher temperature, the catalyst transformed to $Cu_6Mo_5O_{18}$ [16] and remained unchanged up to 500 °C. It was noted that the nominal oxidation state of the Mo ions decreased systematically from +6 ($CuMoO_4$) to +4.8 ($Cu_6Mo_5O_{12}$), which suggested that the gas mixture of CO and H_2O reduced the oxide matrix gradually. The structural patterns for the different phases formed from $CuMoO_4$ during the water–gas shift reaction are displayed in figure 1b.

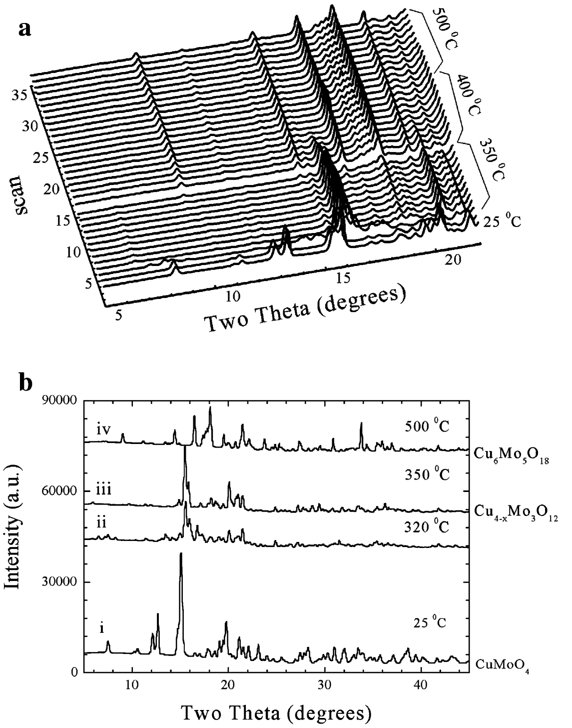

Figure 1. (a) A three-dimensional plot of the TR-XRD patterns (λ = 0.922 Å) acquired during the water–gas shift reaction of a $CuMoO_4$ catalyst. (b) TR-XRD patterns of a $CuMoO_4$ catalyst during different stages of the water–gas shift reaction. (i) at 25 °C; (ii) at 320 °C; (iii) at 350 °C; and (iv) at 500 °C.

Figure 2a shows *in situ* XRD patterns collected during reduction of $CuMoO_4$ with pure hydrogen. It was observed that the diffraction pattern of $CuMoO_4$ collapsed and Cu was the only phase. This is different from the reduction of $CoMoO_4$, where a mixture of $Co_2Mo_3O_8$/$CoMoO_3$ and CoO was observed [17]. Other suboxides such as Mo_4O_{11}, which have been observed during the reduction of MoO_3 [17, 18], were not detected here. It was further seen that the copper phase did not appear until the diffraction lines of the $CuMoO_4$ fully disappeared. The peak width of the Cu diffraction lines decreased after holding the sample at $\sim$ 260 °C for 1 h, pointing to an increase of the Cu particle size. Some additional broad diffraction peaks (marked in figure 2b using asterisks) were also observed in the diffraction

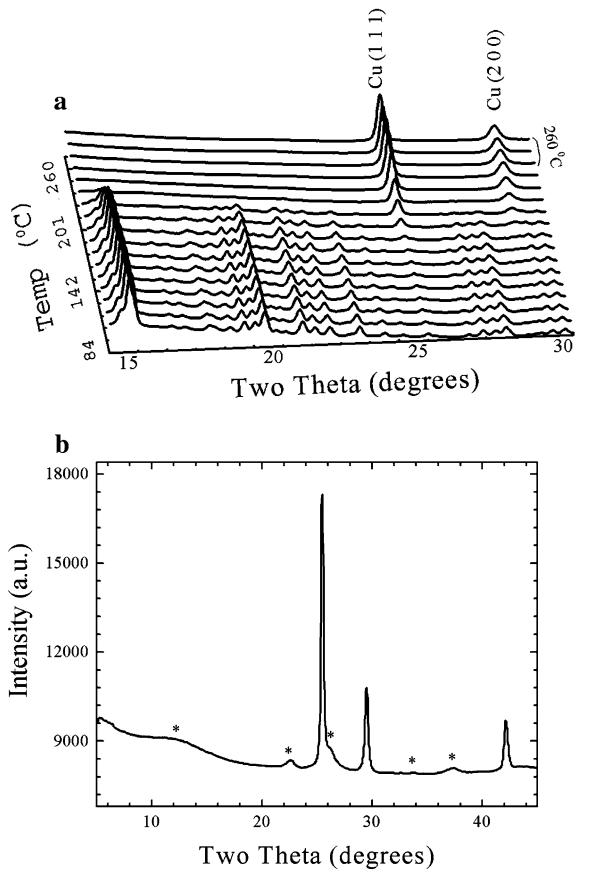

Figure 2. (a) A three-dimensional plot of the TR-XRD patterns (λ = 0.922 Å) of a CuMoO$_4$ or Cu/MoO$_x$ catalyst acquired during different stages of the synthesis process under a flow of 100 % H$_2$. (b) The diffraction pattern of the final product in the reduction process. The diffraction peaks of the unknown phase are marked by asterisks.

pattern of the final product, which suggested the possible existence of other nearly amorphous phases and made an identification impossible. A similar diffraction pattern observed under milder conditions in the reduction of α-NiMoO$_4$ resulted in a mixture of Ni$_4$Mo, Ni and NiO [17]. However, the reduction under pure H$_2$ results in a Ni metal and amorphous phases only, similar to the observation with CuMoO$_4$.

Figure 3 shows the *in situ* TR XRD patterns obtained during the first pass of water–gas shift process that was carried out isothermally at 350, 400 and 500 °C, with a holding time of three hours at each temperature. Around 350 °C, new diffraction peaks appeared that could be indexed to those of Cu$_6$Mo$_5$O$_{18}$ and MoO$_2$. The WGS conditions are less reducing than the synthesis conditions, and it appears that these conditions allow the recrystallization these species from the amorphous mixture. However, the diffraction lines of the copper molybdate disappeared at 500 °C with only the MoO$_2$ phase left in the oxide matrix. It is interesting to note that the Cu$_6$Mo$_5$O$_{18}$ was stable at 500 °C under WGS conditions when the CuMoO$_4$ was not activated with H$_2$. It was also observed that the diffraction lines of the Cu remained unchanged in position during the water–gas shift reaction process.

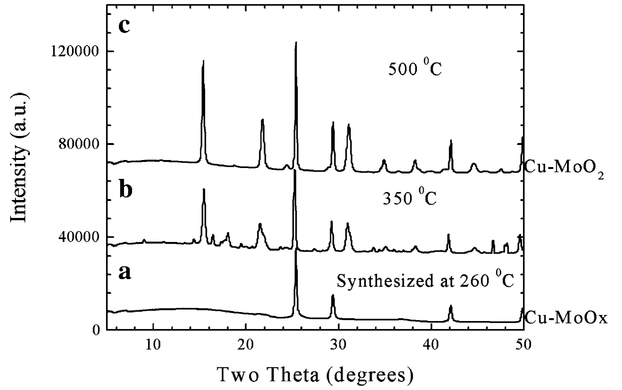

Figure 3. TR-XRD patterns of a Cu/MoO$_x$ catalyst during different stages of the water–gas shift reaction. (a) at 260 °C; (b) at 350 °C; and (c) at 500 °C.

The products of the water–gas shift reaction at 350, 400 and 500 °C are shown in figure 4a. It is clear that the as synthesized catalyst was active around 350 °C. The catalytic activity increased as the temperature was raised to 400 and 500 °C. Our detection set-up was able to detect products (H$_2$, CO$_2$) only at temperatures above

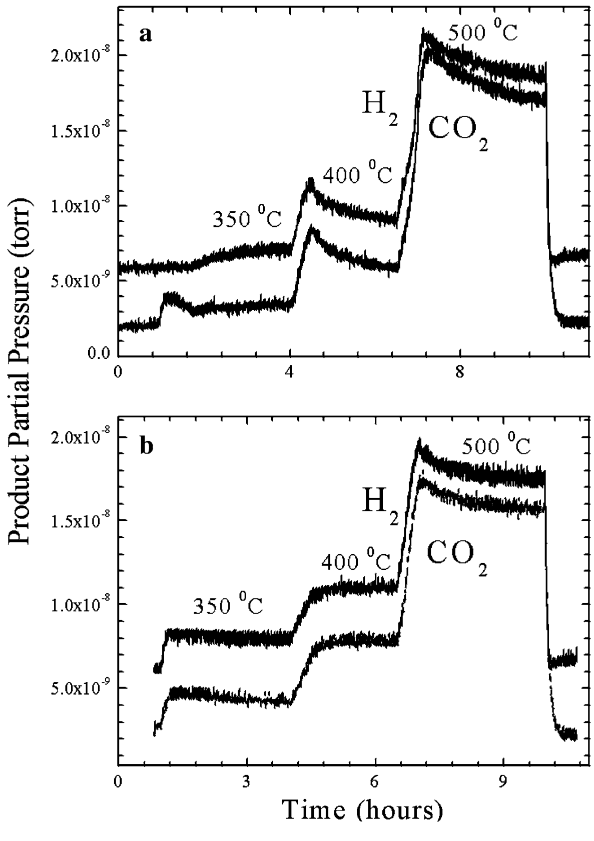

Figure 4. H$_2$ and CO$_2$ concentrations measured for the products of the WGS reaction at different temperatures using the catalyst synthesized at 260 °C. (a) 1st pass. (b) 2nd pass.

300 °C due to the very small amount of catalyst (3–4 mg) in the micro-reactor. It is likely that the reaction also was taken place at temperatures below 300 °C [7].

A second pass of *in situ* TR XRD WGS reaction was performed to determine that the final product Cu–MoO_2 was active at lower temperatures as shown in figure 4b. More significant catalytic activity was observed with relatively stable plateaus around 350, 400 and 500 °C, compared with those observed in figure 4a. The *in situ* XRD data shows that the structure of the two phases, Cu and MoO_2, co-existed and the catalyst remained unchanged during the process of the water–gas shift reaction and in the system.

In order to compare the activity of pure MoO_2 or pure Cu with the synthesized catalyst, *in situ* TR XRD was performed in these catalysts also and the results are displayed in figure 5a and b, respectively. For both materials, large activity was observed around 500 °C. Very little catalytic activity was observed at lower temperature during the water–gas shift reaction process on the Cu metal, while none existed in that of the MoO_2. In figure 5a, we compare the productions of H_2 for our best Cu/MoO_2 catalyst and a Cu catalyst produced after fully reducing CuO [7]. At a temperature of –70 °C, the Cu catalyst was able to adsorb 2–3 times *more* CO than the Cu/MoO_2 catalyst. This implicates a larger number of exposed Cu sites in the pure Cu catalyst. When this is taken into consideration, it is clear that the Cu/MoO_2 catalyst is superior. The bottom panel in figure 5 shows data obtained for the WGS reaction on a Cu(100) single crystal and on model catalysts generated after depositing 0.5 monolayer of Cu on the O-terminated face of zinc oxide, $ZnO(000\bar{1})$, and on a MoO_2 film [19]. These data were obtained in a batch reactor, but they also show that Cu/MoO_2 is more active than pure Cu. This indicates that the Cu–MoO_2 interfacial interaction increases the water–gas shift catalytic activity at temperatures, such as 350 and 400 °C. Each component of the catalyst could be catalyzing different steps of the reaction [1, 3, 4, 7].

Figure 6 shows the rietveld analysis of catalyst C (Cu–MoO_2). The Cu metal was refined to a cubic structure with lattice parameters of $a = b = c = 3.63$ Å and the MoO_2 was refined to a monoclinic structure with $a = 5.64$ Å, $b = 4.87$ Å, $c = 5.64$ Å, $\beta = 120.77°$. The space groups of Cu and MoO_2 were *fm3m* and $p2_1/c$, respectively. These parameters were consistent with those reported in literature for Cu [20, 21] and MoO_2 [22]. The particle sizes of MoO_2 and Cu in the catalysts C are 24.0 nm and 25.2 nm according to the Scherrer equation.

The Mo L_{III}-edge XANES spectra of $CuMoO_4$, MoO_3, plus catalysts A (product of reduction of Cu-MoO_4 in pure H_2 at 260 °C) and C (Cu-MoO_2 at end of pass 1 of WGS) from figure 3 are shown in figure 7a. The spectra of MoO_3 and $CuMoO_4$ exhibited a doublet, which was due to the ligand field split of the 4d orbitals in the Mo ions [23–25]. The separations between these two peaks were 3.05 eV (MoO_3) and 1.91 eV ($CuMoO_4$), which is consistent with the known different coordination environment for these two species. The intensity of the first peak was larger than that of the second one in MoO_3 while the opposite was observed in $CuMoO_4$, which has also been reported in the literature [12, 23], and was fully consistent with an octahedral coordination environment in MoO_3 and a tetrahedral coordination environment in $CuMoO_4$. However, only one broad peak around 2525.2 eV was observed in the Mo L_{III}-edge spectra of catalysts A and C. It was also noted that there was a shoulder peak around 2522.9 eV in the spectrum of catalyst C (Cu–MoO_2).

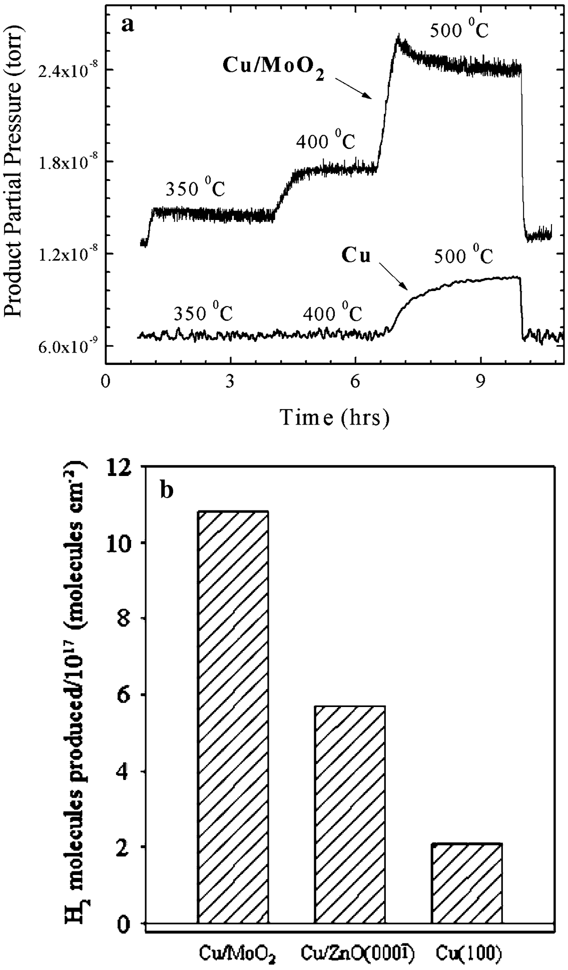

Figure 5. (a) H_2 concentrations measured for the products of the WGS reaction at different temperatures using pure Cu and a Cu/MoO_2 catalyst (from figure 4b). (b) Amounts of H_2 produced during the WGS reaction on 0.5 monolayer of copper deposited on $ZnO(000\bar{1})$ and a polycrystalline MoO_2 film. For comparison is also included the activity of Cu(100). The catalysts were exposed to a mixture of 20 Torr of CO and 10 Torr of H_2O at 350 °C for 5 min in a batch reactor. A reaction time of 2–3 min was enough to reach a steady-state regime in the reactor. The reported values for the amount of H_2 produced are those measured after a reaction time of 5 min [19].

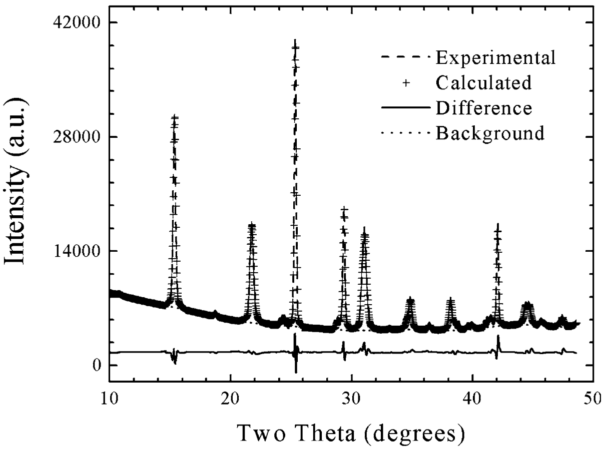

Figure 6. Rietveld analysis of the diffraction pattern of catalyst C. (- - -) Experimental; (+ + +) Calculated; (—) Difference; (...) Background.

Figure 7b shows the first derivative of the Mo L_{III}-edge spectra of $CuMoO_4$, MoO_3, catalysts A and C. The Mo L_{III} edge positions of these four compounds were 2523.5, 2523.4, 2522.3 and 2521.8 eV. The observed energy shift of 1.7 eV was significantly smaller than what have been reported in the Mo K-edge XANES, which was about 10 eV [26], mainly due to less screening effect to the 2p electrons compared with that to the 1s electrons. The Mo L_{III}-edge of catalyst C was 1 eV lower than those of the MoO_3 and $CuMoO_4$, probably due to partial reduction of the Mo ions in the H_2 gas stream. Compared to that of catalyst A, the Mo L_{III}-edge spectrum of the catalyst C shifted slightly to a lower energy position, which suggested that Mo ions were more reduced in the Cu-MoO_2 than those in the catalyst A. Two peaks, which were located around 2522.3 and 2523.5 eV, respectively, were observed in the spectrum of catalyst A. The first peak was very close to that of the Cu–MoO_2 and the second peak was very close to those of the $CuMoO_4$ and MoO_3. This indicated that the original $CuMoO_4$ was partially reduced to MoO_2 in the synthesis process and some $CuMoO_4$ may still exist in the oxide matrix, which has been observed by the *in situ* XRD patterns shown in figure 3. During the water–gas shift reaction, the catalyst A was further reduced and only MoO_2 existed in the oxide matrix.

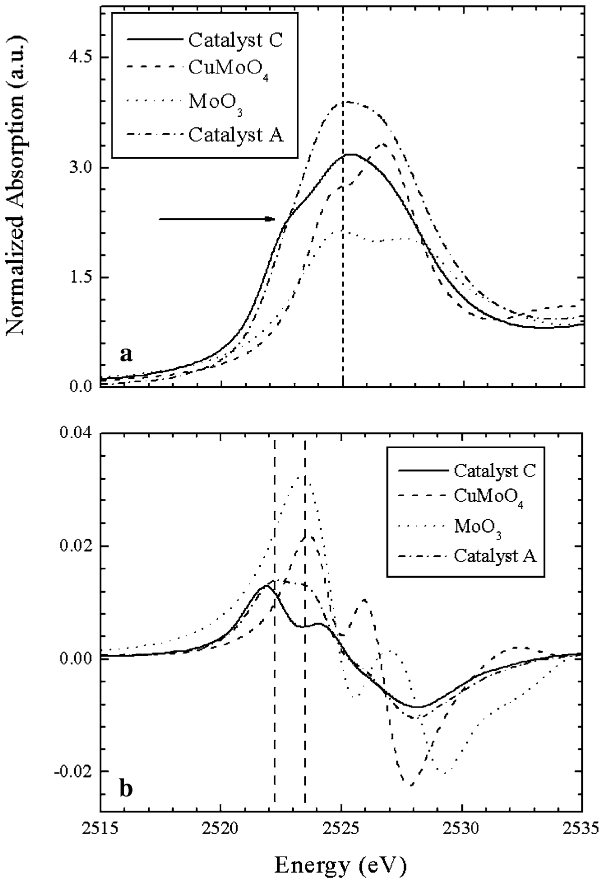

Figure 7. (a) Mo L_{III}-edge XANES spectra of (—) Catalyst C; (- - -) $CuMoO_4$; (...) MoO_3; (–·–·–) Catalyst A. (b) The first derivative of XANES spectra of (—) Catalyst C; (- - -) $CuMoO_4$; (...) MoO_3; (–·–·–) Catalyst A.

The Cu K-edge XANES spectra of $CuMoO_4$, a Cu foil, catalysts A and C are shown in figure 8. It was noted that the Cu K-edge position of the $CuMoO_4$ is at much higher energy position compared with those of the other three species that is mainly ascribed to the high oxidation state of the Cu ions. A pre-edge was observed in the spectrum of $CuMoO_4$, which was due to an electronic transition from the Cu 1s orbitals to the Cu 3d orbitals. This transition was dipole forbidden while quadruple allowed and could also be explained by the hybridization of the 2p orbitals of the oxygen and the 3d orbitals of the Cu ions [27, 28]. The XANES spectra of the other three compounds were similar and showed a peak around 8983.1 eV. However, in the Cu K-edge spectrum of the catalyst A, the peak around 8983.1 eV was broad and was slightly different from those of the

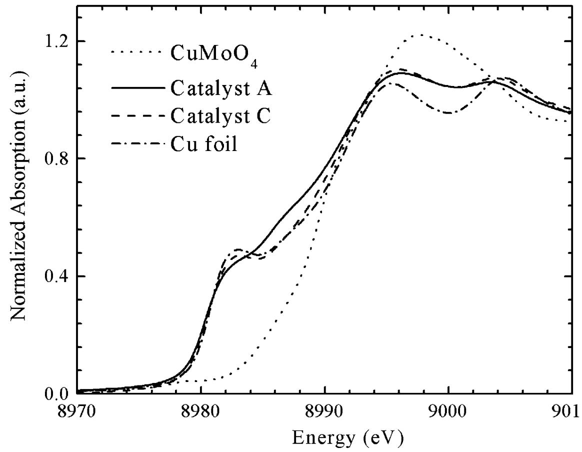

Figure 8. Cu K-edge XANES spectra of (...) $CuMoO_4$; (—) Catalyst A; (- - -) Catalyst C; (–·–·–) Cu foil.

Cu foil and catalyst C, where a sharp peak was observed instead. This observation was consistent with the Mo L$_{III}$-edge spectra presented in figure 7, where some copper molybdate was still left in the oxide matrix in catalyst A. However, the amorphous material of catalyst A is composed by very small amount of copper molybdate and didn't shift the Cu K-edge significantly compared with that of the catalyst C.

4. Conclusions

The structural transformations of CuMoO$_4$ and Cu–MoO$_2$ catalysts during H$_2$ reduction and the water–gas shift reaction were followed by *in situ* time-resolved XRD. During the synthesis process of Cu–MoO$_2$, metallic Cu was formed from CuMoO$_4$ around 260 °C, with the co-existence of amorphous molybdenum oxide and copper molybdate. Under the water–gas shift reaction, Cu$_6$Mo$_5$O$_{18}$ and MoO$_2$ co-existed at 350 °C and Cu$_6$Mo$_5$O$_{18}$ transformed to additional Cu–MoO$_2$ at higher temperature. Significant water–gas shift activities were observed at a temperature of 350 °C and increased with the raise of temperature. The catalytic activities originated from interfacial interactions between Cu clusters and MoO$_2$.

Acknowledgments

This work was supported by the U.S. Department of Energy, Office of Basic Energy Sciences, Chemical Science Division (DE-AC02–98CH10886). The NSLS is supported by the Chemical and Materials Science Divisions of the U.S. Department of Energy.

References

[1] R. Burch, Phys. Chem. Chem. Phys. in press.
[2] M.S. Spencer, Top Catal 8 (1999) 259.
[3] G. Jacobs, E. Chenu, P.M. Patterson, L. Williams, D. Sparks, G. Thomas and B.H. Davis, Appl. Catal. A 258 (2004) 203.
[4] W. Liu and M. Flytzani-Stephanopoulos, J. Catal. 153 (1995) 304.
[5] A.N. Koryabkina, A.A. Phatak, F.W. Ruettinger, J.R. Farrauto and H.F. Ribeiro, J. Catal. 217 (2003) 233.
[6] X. Wang, J. Rodriguez, J. Hanson, D. Gamarra, A. Martínez-Arias and M. Fernández-Garcia, J. Phys. Chem. B 109 (2005) 19595.
[7] X. Wang, J.A. Rodriguez, J.C. Hanson, D. Gamarra, A. Martinez-Arias and M. Fernandez-Garcia, J. Phys. Chem. B 110 (2006) 428.
[8] X. Wang, J.C. Hanson, A.I. Frenkel, J.Y. Kim and J.A. Rodriguez, J. Phys. Chem. B 108 (2004) 13667.
[9] J.Y. Kim, J.A. Rodriguez, J.C. Hanson, A.I. Frenkel and P.L. Lee, J. Am. Chem. Soc. 125 (2003) 10684.
[10] B.H. Toby, J. Appl. Cryst. 34 (2001) 210.
[11] A.C. Larson and R.B. Von Dreele, Los Alamos National Laboratory Report LAUR (2000) 86.
[12] J.A. Rodriguez, S. Chaturvedi, J.C. Hanson, A. Albornoz and J.L. Brito, J. Phys. Chem. B 102 (1998) 1347.
[13] J.A. Rodriguez, S. Chaturvedi, J.C. Hanson and J.L. Brito, J. Phys. Chem. B 103 (1999) 770.
[14] M. Newville, B. Ravel, D. Haskel, J.J. Rehr, A.E. Stern and Y. Yacoby, Phys. B 154 (1995) 208.
[15] E. McCarron and J. Calabrese, J. Solid State Chem. 65 (1986) 215.
[16] L. Katz, A. Kasenally and L. Kihlborg, Acta Cryst. B 27 (1971) 2071.
[17] J.A. Rodriguez, J.Y. Kim, J.C. Hanson and J.L. Brito, Catal. Lett. 82 (2002) 103.
[18] T. Ressler, R.E. Jentoft, J. Wienold, M.M. Günter and O. Timpe, J. Phys. Chem. B 104 (2000) 6360.
[19] M. Pérez, J. Evans, J.M. Araujo and J.A. Rodriguez, to be published.
[20] G. Waldo, Am. Mineral. 20 (1935) 59.
[21] W.P. Davery, Phys. Rev. 25 (1925) 753.
[22] B.G. Brandt and A.C. Skapski, Acta Chem. Scand. 21 (1967) 661.
[23] E.J. Lede, F.G. Requejo, B. Pawelec and J.L.G. Fierro, J. Phys. Chem. B 106 (2002) 7824.
[24] S.R. Bare, Langmuir 14 (1998) 1500.
[25] J.G. Chen, Surf. Sci. Rep. 30 (1997) 1.
[26] G.N. George, W.E. Cleland Jr., J.H. Enemark, B.E. Smith, C.A. Kipke, S.A. Roberts and S.P. Cramer, J. Am. Chem. Soc. 112 (1990) 2541.
[27] W. Wen, B. Kumarasamy, S. Mukerjee, M. Auinat and Y. Ein-Eli, J. Electrochem. Soc. 152 (2005) A1902.
[28] M. Giorgetti, S. Passerini, W.H. Smyrl, S. Mukerjee, X.Q. Yang and J. McBreen, J. Electrochem. Soc. 146 (1999) 2387.